Study of electrodeposition of $(Bi,Sb)_2Te_3$ nanowires by voltammetric methods and electrochemical impedance spectroscopy

M. SIMA[a], E. VASILE[b], MARIANA SIMA[a]
[a]*National Institute of Materials Physics, P.O. Box MG 7, 077125 Magurele, Romania*
[b]*METAV-CD, 31 CA Rosetti Street, 020015 Bucharest, Romania*

Nanostructured thermoelectric semiconductors are a promising material to convert waste heat to electricity for energy regeneration due to improvement of Seebeck coefficient and thermal conductivity reducing. Among various thermoelectric materials, bismuth telluride based alloys are the most used in the fabrication of TE devices. The processes associated with the electrodeposition of $(Bi,Sb)_2Te_3$ nanowires and films are reported along with an analysis of the composition, morphology and structure of resulting materials. Electrochemical behavior was examined using cyclic and linear voltammetry and electrochemical impedance spectroscopy techniques.

(Received November 1, 2011; accepted November 23, 2011)

Keywords: Electrodeposition, Semiconductor, Nanowires, Thermoelectric

1. Introduction

Thermoelectric devices generate an electric potential gradient from a thermal gradient, or vice versa, without any actuating parts. The improvement of thermoelectric devices efficiency is connected with the increase of thermoelectric performance of the materials used to their fabrication. The performance of a thermoelectric material is represented by the dimensionless figure of merit, $ZT=S^2\sigma T/\kappa$, where S, σ, κ and T are Seebeck coefficient, the electrical conductivity, the thermal conductivity and the temperature in Kelvin, respectively. Nanostructured thermoelectric semiconductors [1-9] are a promising material to convert waste heat to electricity for energy regeneration due to improvement of Seebeck coefficient and thermal conductivity reducing. $Bi_{0.5}Sb_{1.5}Te_3$ is one of the most used thermoelectric materials for applications at temperatures close to room temperature; it is a p-type semiconductor and is synthesized by several methods among which the electrochemical method. Thermal conductivity of $Bi_{2-x}Sb_xTe_3$ system decreases with increasing content in Sb_2Te_3, reaching a minimum when the molar concentration Sb_2Te_3 reach 70%; on the other hand, the mobility of holes increases in the new p-type semiconductor by adding Sb_2Te_3 [10]. Seebeck coefficient for bulk $Bi_{2-x}Sb_xTe_3$ system can reach values of 260μV/K. Electrochemical method allows the growth of uniform films with thickness from nanometric values at a few millimeters over large areas. By varying the composition of the solutions and electrode potential one can prepare films with different compositions. Among the deposition techniques, the electrodeposition is the cheapest to manufacture nanostructured materials and miniaturized devices due to its operation at low temperatures and without vacuum requirements, high deposition rate and easy transition from one size to another.

In this paper, the electrochemical synthesis of $(Bi,Sb)_2Te_3$ nanowire array from nitrate solution was investigated using cyclic and linear voltammetry and electrochemical impedance spectroscopy.

2. Experimental

Electrochemical characterization was conducted potentiostatically in a conventional three-electrode cell configuration at room temperature. Platinum and a commercial saturated calomel electrode (SCE) were used as the counter and reference electrode, respectively. Stainless steel and platinum foils and a track etched membrane (polycarbonate membrane) were used as working electrode to investigate the electrochemical growth of $Bi_{2-x}Sb_xTe_3$ film and wires. Prior electrodeposition, polycarbonate membrane with a thickness of 27μm, pore diameter of about 500 nm and 10^8 cm^{-2} pores density was covered by sputtering with a thin gold film; this film was thickened by electrochemical deposition of a copper layer. Pulsed electrodeposition based on the variation of the current over time was used to prepare $Bi_{2-x}Sb_xTe_3$ films and wires. The Bi-Sb-Te ternary solution was prepared by dissolution of $Bi(NO_3)_3.5H_2O$ and TeO_2 in concentrated HNO_3 and $SbCl_3$ in tartaric acid aqueous solution and mixing of the two solutions; the final composition of the solution was 9.39mM $HTeO_2^+$, 1.82mM Bi^{3+}, 5.69mM SbO^+, and 37.9mM tartaric acid in 1M HNO_3. For SEM and XRD measurements of the prepared nanowires, after the electrodeposition process the polymer membrane was dissolved in dichloromethane.

The electrochemical measurements were carried out with an Autolab PGSTAT 30 potentiostat/galvanostat connected to a computer. Electrochemical impedance spectroscopy (EIS) tests were carried out in 10^{-2} Hz ≤ f ≤ 10^{6} Hz frequency range with an *ac* voltage amplitude of ±5 mV. These spectra were interpreted on the basis of equivalent electric circuits using specialized fitting software, ZView 2.90c. The semiconductor films and wires were imaged using a field emission scanning electron microscope Quanta InspectF equipped for chemical composition measurements with an EDX device from EDAX. X-ray diffraction (XRD) analyses were performed on a Bruker D8 Advance type X-ray diffractometer, in focusing geometry, equiped with copper target X-ray tube and LynxEye one-dimensional detector.

3.Results and discussion

3.1.Cyclic and linear voltammetry analyses

Electrochemical behavior of the solution containing Bi^{3+}, $HTeO_2^+$ and SbO^+ at 11^0C ions was examined by cyclic and linear voltammetry using as working electrodes platinum and stainless steel foils and a Cu/Au/polycarbonate membrane; the results are shown in Fig.1.

Working at a temperature lower than room temperature allows obtaining adherent $Bi_{2-x}Sb_xTe_3$ deposits. In the Fig.1, it can be seen a small reduction wave, between 0.4 and 0V on voltammogram (a) or between 0.22 and -0.03V on voltammogram (b); this peak was attributed to the reduction of the ions to Te element and $Bi_{2-x}Sb_xTe_3$ compounds [11]. The pronounced peaks at -0.157V (Fig.1, a) or -0.187V (Fig.1,b) are related to the formation of Sb element. The waves observed on the anodic branch of the voltammograms (at 0.168, 0.47 and 0.57V on curve (a) and at 0.197, 0.45 and 1.17V on curve (b) are in connection with the oxidation of Sb and Bi on top of $Bi_{2-x}Sb_xTe_3$ film and oxidation of $Bi_{2-x}Sb_xTe_3$ to Sb and Bi; in the case b, the shift of the oxidation potential of $Bi_{2-x}Sb_xTe_3$ to 1.17V could be attributed to chemical reaction between stainless steel substrate and deposit.

Fig1.c shows linear voltammogram of the electrodeposition process of $Bi_{2-x}Sb_xTe_3$ compounds into the pores of the polycarbonate membrane. The two reduction waves observed on this voltammogram during cathodic scan are located between -0.04 and -0.27V with peaks at -0.191 and -0.255V. The shift of these reduction waves to more cathodic potential is due to diffusion process of the ions into the membrane pores. The assignment of the waves is similar to those from the voltamogramms (a) and (b) from Fig.1.

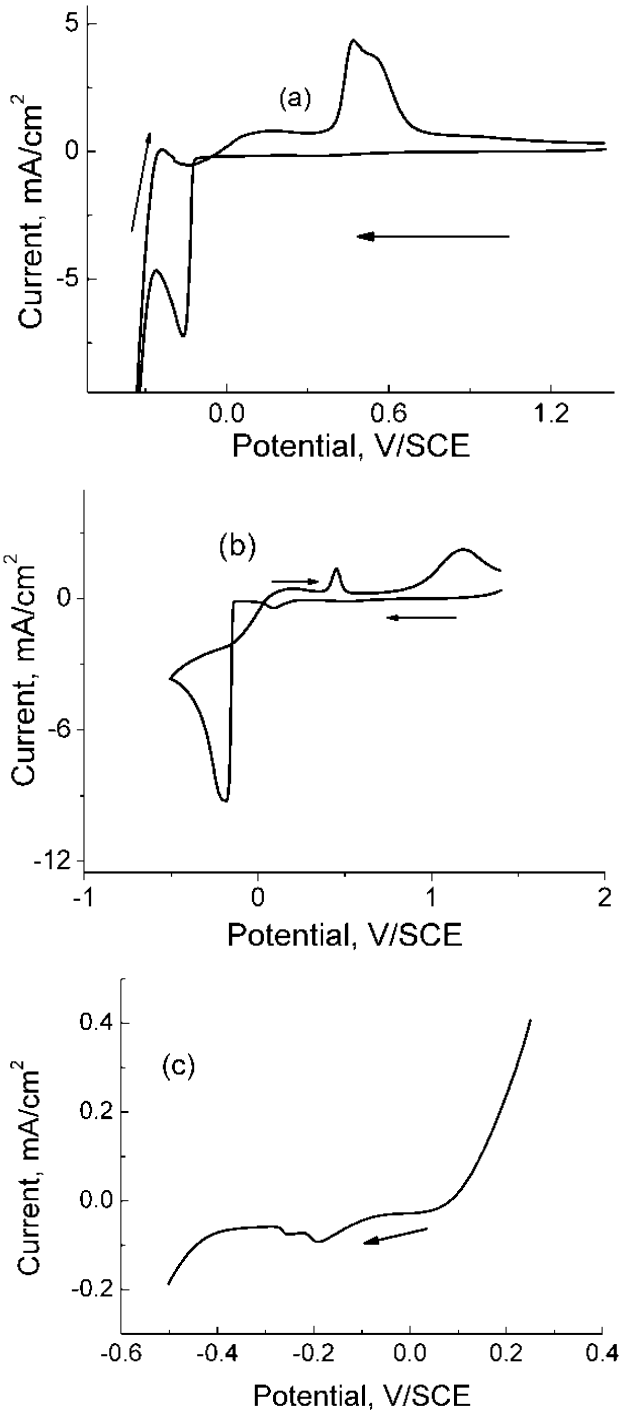

Fig.1. Cyclic voltammograms of platinum (a) and stainless steel (b) foils and linear voltammogram of Cu/Au/polycarbonate membrane (c) in aqueous solution containing Bi^{3+}, $HTeO_2^+$ and SbO^+ ions at 11^0C; scan rate 50mV/s.

3.2. EIS analyses

3.2.1.Growth of $Bi_{2-x}Sb_xTe_3$ film on stainless steel foil

EIS has been regarded as a tool for obtaining more information about the kinetics of reduction process. We investigated by EIS the electrodeposition process of $Bi_{2-x}Sb_xTe_3$ at stainless steel electrode in nitric acid solution at a potential where the Bi-Sb-Te ternary film is deposited. The Nyquist diagrams (Fig.2,a) of the stainless steel electrode, recorded at a potential of -0.11V present an incomplete semicircle in the region of high frequencies (most obvious at low temperatures), attributed to charge transfer and a straight line inclined to 45^0 due to diffusion process that curves at low frequencies (this behavior is attributed to irregular surface of the electrode).

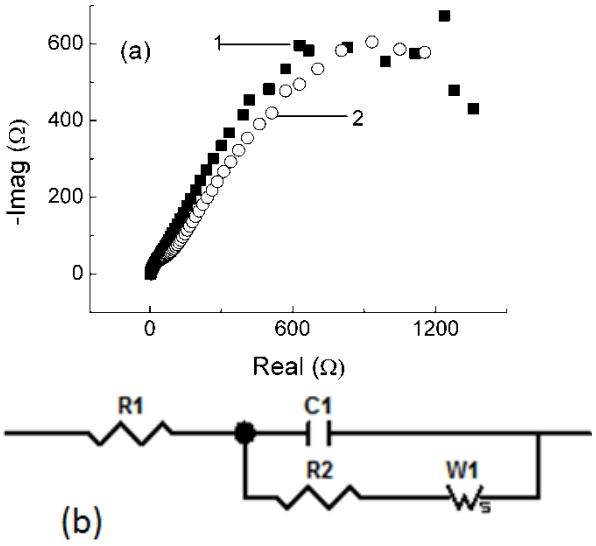

Fig. 2. (a) Nyquist diagram for stainless steel electrode in the electrodeposition solution at -0.11Vand (1) room temperature and (2) 11 ^{0}C; (b) the equivalent electric circuit used to fit the impedance spectra from Fig. 2,a.

Charge transfer occurs during the reducing process of $HTeO_2^+$ species at tellurium element, which combines in a later stage with bismuth and antimony ions on the electrode surface.

$$HTeO_2^+ + 3H^+ + 4e^- \rightarrow Te + 2H_2O \quad (1)$$

$$3Te + 2Bi^{3+} + 6e^- \rightarrow Bi_2Te_3 \quad (2)$$

$$3Te + 2Sb^{3+} + 6e^- \rightarrow Sb_2Te_3 \quad (3)$$

The experimental results were fitted using the equivalent electric circuit shown in Fig.2,b, corresponding to the two different time constants. Table I contains the values of the equivalent circuit elements.

Table 1. Values of the equivalent circuits parameters

Circuit elements		$(Bi,Sb)_2Te_3$ film at room temperature (Fig.2)	$(Bi,Sb)_2Te_3$ film at 11^0C (Fig.2)	$(Bi,Sb)_2Te_3$ wires (Fig.3)
R1, Ω		3.26	5.17	4.00
R2, Ω		1	31.07	0.32
R3, Ω				21.17
W1	R, Ω	1475	1539	60.56
	τ,s	15.23	27.57	20.77
	P	0.5	0.5	0.32
CPE1	$T, \Omega^{-1}s^P$			0.0046
	P			0.59
C1, F		0.000013	0.000047	0.000021

The first time constant is determined by the charge transfer resistance, R2, in parallel with the double layer capacitance represented by a capacitance, C1. R1 is a ohmic resistance which depends on the conductivity of the electrolyte. The second time constant is described by Warburg impedance (W1) associated with the diffusion process.

Generalized finite Warburg element proposed by Macdonald [12] and depicted by the equation (4) is an extension of the finite length Warburg element, which is the solution of the one-dimensional diffusion equation of a particle. For this last element P=0.5.

$$Z_W = R\,\frac{\tanh(i\tau\omega)^P}{(i\tau\omega)^P}, \quad (4)$$

where $i=\sqrt{-1}$, τ is the time constant associated with the diffusion process, ω is angular frequency, R represents a diffusion impedance component independent of frequency and P – an exponent taking values between 0 and 1. The data from the Table I show that charge transfer resistance and the diffusion impedance values increase at lower temperatures than room temperature; also increases the capacity of double layer.

3.2.2. Growth of $Bi_{2-x}Sb_xTe_3$ wires into the pores of a polycarbonate membrane

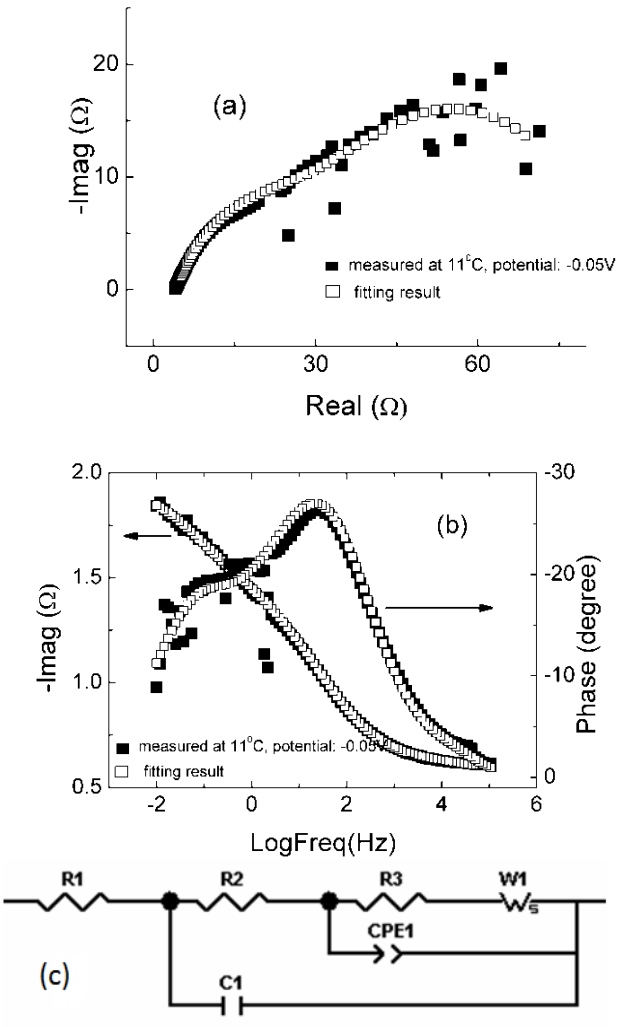

Fig. 3. Nyquist (a) and Bode (b) diagrams for Cu/Au/membrane electrode in the electrodeposition solution at -0.05V; c) the equivalent electric circuit used to fit the impedance spectra from Fig.3.

The Nyquist plot obtained for Cu/Au/membrane electrode at -0.05V shows two time constants, the first relating to the charge transfer process typical of electrolyte/electrode interface (semicircle at high frequencies) and another to space limited diffusion due to the finite volume of the membrane pores and corresponding to a sloping capacitive line extends to low frequency (Fig.3). The first time constant is determined by the charge transfer resistance, R3, in parallel with the double layer capacitance represented by a constant phase element, CPE1. The second time constant is described by the membrane capacitance C1 and the pore resistance R2. The Warburg impedance (W1) is associated with diffusion phenomena into the membrane pores. Table I contains the values of the equivalent circuit elements. Here, the capacitance of double layer was described using a constant phase element, CPE1 because electrode surface is more irregular and more changeable. The impedance of this CPE component is described by the equation (5) [13]:

$$Z(CPE) = \frac{1}{T\ (i\omega)^P} \tag{5}$$

where the T value obtained by experimental data fitting is associated with double layer capacitance and exponent P takes values between 0 and 1.

Charge transfer resistance and the diffusion impedance values for Cu/Au/membrane electrode (Table I) are lower compared to the corresponding values for stainless steel electrode (at low temperature); in this case the growth process of $Bi_{2-x}Sb_xTe_3$ wires into membrane pores could be faster.

3.3. $Bi_{2-x}Sb_xTe_3$ film and nanowires preparation

It was observed that films obtained using the direct mode [14], particularly antimony ternary compounds, have significant roughness and present defaults and cracks. In order to improve their morphology, it was applied pulse plating [15] (t_{on}=5s, J_c=-2mA cm^{-2}, t_{off}=5s, for $Bi_{2-x}Sb_xTe_3$ film growth and t_{on}=5s, J_c=-0.1mA cm^{-2}, t_{off}=5s, for $Bi_{2-x}Sb_xTe_3$ wires growth). The cathodic reduction process of ions induced the deposition of $Bi_{2-x}Sb_xTe_3$ tubes (Fig.4,a,b) with a composition (at%): Bi-6.2, Sb-21.7, Te-72.1; the length of the tubes was of about 12μm. The composition of $Bi_{2-x}Sb_xTe_3$ film with globular structure deposited on stainless steel support (Fig.4,c) was (at%): Bi-14.6, Sb-12.5, Te-72.9.The X-ray diffraction patterns of $Bi_{2-x}Sb_xTe_3$ film and tubes (Fig. 5) prepared by pulse plating show the characteristic peaks of $Bi_2Sb_2Te_3$ and $Bi_{0.5}Sb_{1.5}Te_3$ compounds, respectively.

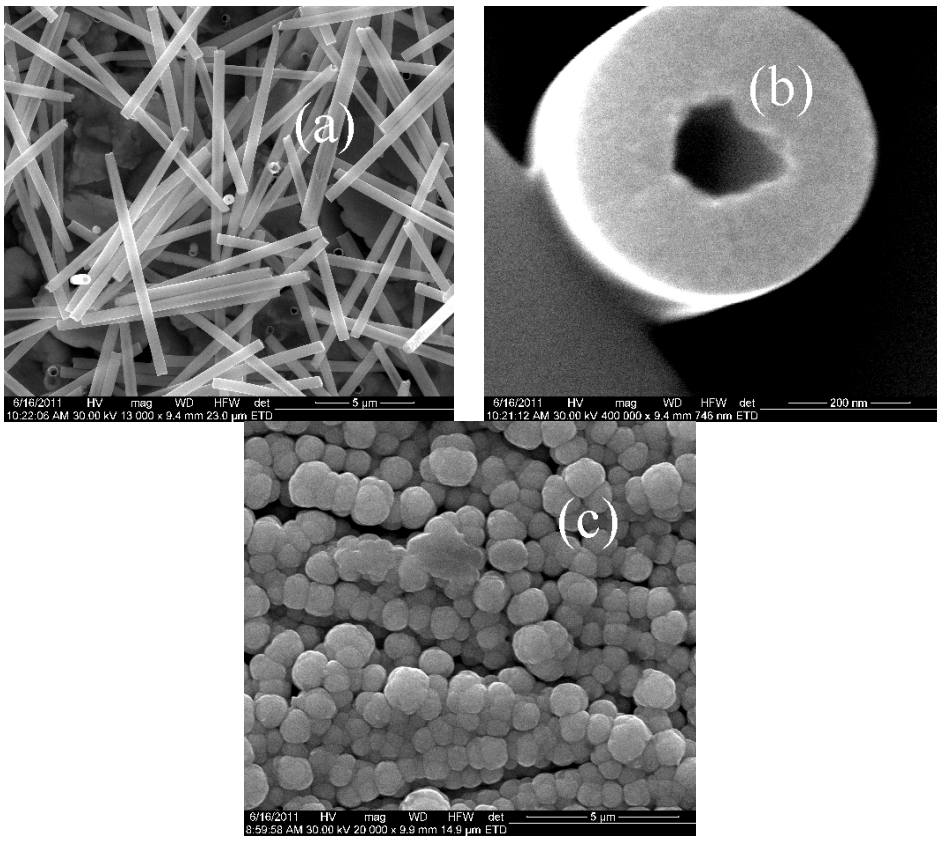

Fig.4. SEM images of $Bi_{2-x}Sb_xTe_3$ tubes (a,b) and film on stainless steel support (c) prepared at 11^0C by pulse plating

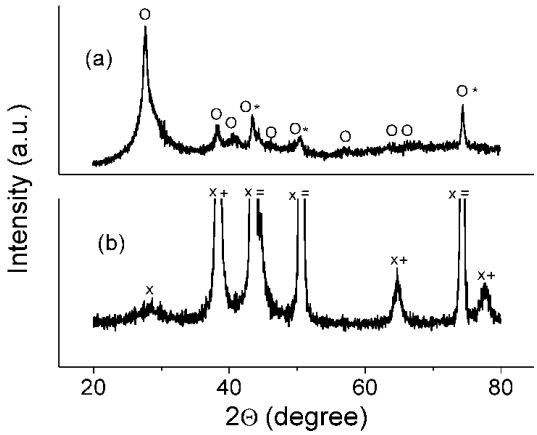

Fig.5. XRD patterns of: a) $Bi_2Sb_2Te_3$ film (O) on stainless steel foil (Fe); b) $Bi_{0.5}Sb_{1.5}Te_3$ nanotubes (X) on Au (+)/Cu (=) support.*

4. Conclusions

The electrochemical behavior of a mixture of bismuth, antimony and tellurium ions was investigated in nitric acid solution, using as working electrodes platinum and stainless steel foils and a Cu/Au/polycarbonate membrane. The results show the formation of $Bi_{2-x}Sb_xTe_3$ at slightly cathodic potentials; at potential values more negative than -0.15V /SCE takes place deposition in excess of antimony element. A good morphology of the deposits was obtained at a temperature lower than room temperature. Current pulse plating was used to prepare $Bi_{2-x}Sb_xTe_3$ film and tubes with the compositions (at%): Bi-14.6, Sb-12.5, Te-72.9 and Bi-6.2, Sb-21.7, Te-72.1.

Acknowledgement

This work was supported by UEFISCDI, project number 72155 PNII-Partnerships/2008

References

[1] J.R. Lim, J.F.Whitacre, J-P. Fleurial, C-H. Huang, M.A. Ryan, N.V. Myung, Adv. Mater. **17**, 1488 (2005)
[2] M. N. Touzelbaev, P. Zhou, R. Venkatasubramanian, K. E. Goodson, J. Appl. Phys. **90**, 763 (2001).
[3] J. C. Caylor, K. Coonley, J. Stuart, T. Colpitts, R. Venkatasubramanian, Appl. Phys. Lett. **87**, 23105 (2005).
[4] H. Beyer, J. Numus, H. Böttner, A. Lambrecht, E.Wagner, G. Bauer, Physica E **13**, 965 (2002).
[5] A. I. Hochbaum, R. Chen, R. D. Delgado, W. Liang, E. C. Garnett, M. Najarian, A. Majumdar, P. Yang, Nature **451**, 163 (2008).
[6] A. I. Boukai, Y. Bunimovich, J. Tahir-Kheli, J.-K. Yu, W. A. Goddard III, J. R. Heath, Nature **451**, 168 (2008).

[7] G. J. Snyder, T. Caillat, J.-P. Fleurial, Phys. Rev. B **62**, 10185 (2000).
[8] D. G. Cahill, S. K. Watson, R. O. Pohl, Phys. Rev. B **46**, 6131 (1992).
[9] J. Weber, K. Potje-Kamloth, F.Hasse, P. Detemple, F. Volklein, T.Doll, Sens. Actuator A;Phys. **132**, 325 (2006).
[10] G.S.Nolas, J. Sharp, H.J. Goldsmid, Thermoelectrics-Basic Principles and New Materials Developments, Springer 2001, p125.
[11] F-H Li, Q-H Huang, W.Wang, Electrochim. Acta **54**, 3745 (2009).
[12] J.R. Macdonald, Impedance Spectroscopy, Wiley 1987, p.122.
[13] J.R. Macdonald, Impedance Spectroscopy, Wiley 1987, p 90.
[14] M.Sima, E.Vasile, Mariana Sima, Optoelec. Adv. Mat.-Rapid Commun **3**, 539-542 (2009)
[15] V.Richoux, S.Diliberto, C. Boulanger, J. Electron,Mater. **39**, 1914 (2010).

*Corresponding author: msima@infim.ro